

Trajectory Planning with Adaptive Control Primitives for Autonomous Surface Vehicles Operating in Congested Civilian Traffic

Brual C. Shah¹, *Student Member, IEEE*, Petr Švec¹, *Member, IEEE*, Ivan R. Bertaska², Wilhelm Klinger²,
Armando J. Sinisterra², Karl von Ellenrieder², *Member, IEEE*, Manhar Dhanak², and
Satyandra K. Gupta³, *Senior Member, IEEE*

Abstract—We introduce a model-predictive trajectory planning algorithm for unmanned surface vehicles (USVs) operating in congested civilian traffic. The planner reasons about the availability of contingency maneuvers needed in case of any of the civilian vessels breaches the International Regulations for the Prevention of Collisions at Sea (COLREGs). Our exploratory study indicated that implementing the envisioned planner requires significant speed up of trajectory planning to cope with the dynamics of the scene, and evaluation of collision risk. We describe a new method for efficiently searching 5D state space for a dynamically feasible trajectory using adaptive control action primitives. The algorithm estimates the congestion of the state space regions to evaluate collision risk, and then dynamically scales action primitives used during the search while preserving their dynamical feasibility. Our simulation experiments demonstrate that this leads to a substantial increase in the search efficiency and a decrease in the number of collisions, especially in complex scenarios with a higher number of civilian vessels.

I. INTRODUCTION

Unmanned surface vehicles (USVs) [1] are increasingly being used in search and rescue, harbor surveillance, hydrologic survey, and defense tasks [2]. However, their capability to operate fully autonomously near harbor areas with significant traffic is still highly limited because of the wide range of dynamic response characteristics exhibited by civilian boats. In addition, the maneuvers executed by the USVs create a reciprocal relationship between them and the civilian vessels, as well as, between civilian vessels. In complex multi-vehicle operational scenarios, this may lead to cascades of collisions if standardized collision avoidance rules are not followed.

The International Regulations for the Prevention of Collisions at Sea (COLREGs) [3] were developed to prescribe allowable maneuvers for marine vessels. In recent years, efforts have been made to incorporate the regulations into autonomous systems [4], [5], [6] (see Fig. 1 that shows an experiment performed by the authors). However, the current state-of-the-art unmanned systems can operate safely only in

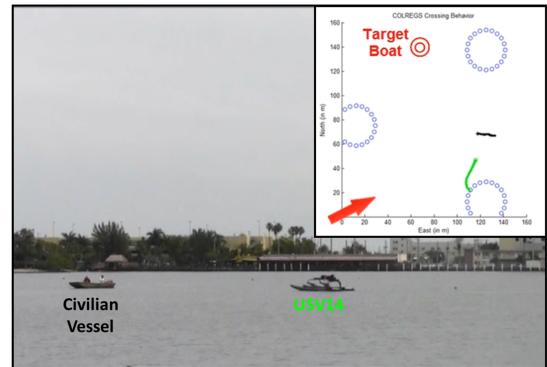


Fig. 1: The USV14 autonomously avoiding a civilian vessel according to COLREGs in a crossing-from-right scenario [6].

simple scenes with civilian vessels that follow COLREGs. The assumption that every vessel follows the rules and have the same amount of information about the states of other vessels makes the problem trivial.

Let us consider the scenario shown in Fig. 2. All the vessels are assumed to follow COLREGs while pursuing their way out of the port. The USV enters the harbor from the south channel with the objective to reach the north channel by yielding to other civilian vessels according to COLREGs. During its motion, the USV encounters a “crossing from right situation” (Rule 15) with respect to civilian vessel 1 (CV1). The CV1 has the right of way and is assumed to maintain its course with the same speed and heading. The USV should perform a “give-way” maneuver in order to yield to CV1. The CV2 needs to give way to CV3 and CV4, as it encounters the “crossing from right” and the “head on” (Rule 14) situation, respectively. Similarly, CV3 will need to yield to CV4 and CV4 can continue straight to the east channel provided that the USV yields to CV1.

There is a considerable collision risk between the USV and CV1 if CV1 slows down and swerves left under an incorrect assumption that the USV will decide to steer sharp left to avoid a collision with the coast on its starboard and the vessel. This situation may occur if CV1 incorrectly interprets the scenario due to the underestimation of the USV’s size, heading, speed, distance, and the clearance between the USV and the coast. In such a situation, it may be in the USV’s best interest to actually breach COLREGs by turning left to avoid a collision. However, this could cause a chain reaction

¹B. Shah and P. Švec are with the Department of Mechanical Engineering, University of Maryland, College Park, MD 20742, USA {brual, petršvec}@umd.edu

²I.R. Bertaska, W. Klinger, A.J. Sinisterra, K. Ellenrieder, and M. Dhanak are with the Department of Ocean & Mechanical Engineering, Florida Atlantic University, Dania Beach, FL 33004-3023, USA {ibertaska, wklinger, asiniste, ellenrie, dhanak}@fau.edu

³S.K. Gupta is with the Department of Mechanical Engineering and Institute for Systems Research, University of Maryland, College Park, MD 20742, USA skgupta@umd.edu

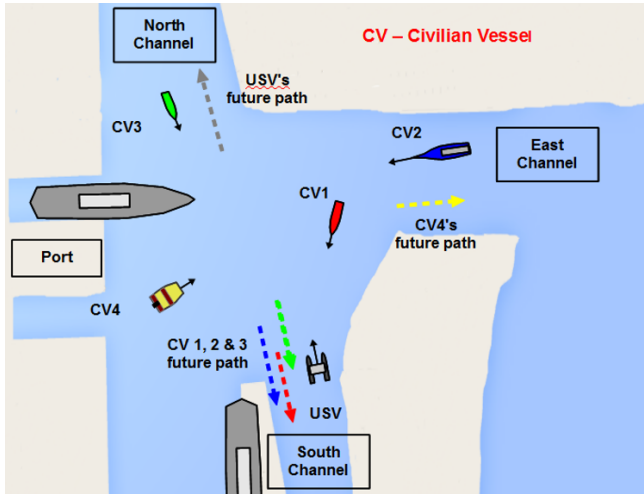


Fig. 2: A scenario with an USV and civilian vessels moving to their respective destinations in a harbor region.

leading to multiple collisions as the USV's dynamics and natural forces may affect its ability to slow down and turn sharply on time. For example, CV4's assumption of the USV following COLREGs would become voided, and thus force the vessel to turn left to avoid a collision. This in turn would endanger CV3 and the chain of contingencies would evolve.

Despite the outlined challenges, the trajectory planning algorithms of future unmanned systems capable of long-term autonomy will need to reason about the associated risk of collision, and the availability of contingency maneuvers when any of the civilian vessels breaches COLREGs. The traditional lattice based planners [7], [8] that utilize a fixed set of action primitives will not work effectively in congested and dynamic scenes. This is because control primitives with long time scales lead to fast trajectory planning, but these cannot be used in congested traffic. On the other hand, control primitives with short time scales can be used to compute efficient trajectories in congested traffic, but long planning time will make them obsolete as the scene will change significantly after the planning is completed. The right combination of long and short time scale control primitives is required to achieve a balance between planning and trajectory efficiency, while minimizing the collision risk.

We have developed a new approach (see Section IV-F) for adapting action primitives time scales based on the degree of congestion, and integrated these primitives into a lattice-based trajectory planner that computes trajectories in 5D state space, and accounts for collision risk and availability of contingency maneuvers (see Section IV). This approach enables us to successfully find trajectories in congested scenes where trajectory planning based on fixed scale primitives does not perform well. Section V demonstrates that this leads to a significant improvement in the performance of the planner and lower incidence of collisions compared to a baseline, Velocity Obstacles (VO) based, COLREGs-compliant planner [5].

II. RELATED WORK

The up-to-date review of research articles that present reactive and deliberative trajectory planning techniques [2], [7], [8], [9] for USVs and ships, including those that incorporate COLREGs into planning, can be found in [10], [4].

The reactive approaches compute collision avoidance maneuvers in respect to vessels that are only in the close vicinity to the USV. They do not employ advance reasoning about their behaviors. For example, Tan et al. [11] solves the collision avoidance in accordance with COLREGs by choosing an appropriate maneuver from a list of candidate maneuvers using a prioritized list of predefined criteria. Benjamin et al. [12] develops a set of COLREGs-compliant obstacle avoidance (OA) behaviors in an interval programming (IP) based behavior architecture. Other approaches for COLREGs-compliant autonomous guidance include a fuzzy logic based technique in [13], and a technique [14] that adapts artificial potential fields. These local approaches, however, may lead to highly inefficient and possibly risky USV's operation in congested environments as they do not reason multiple steps ahead. This can prove fatal and lead to a series of collisions. Hence, a deliberative planning approach that employs sequential search is required.

Several COLREGs-compliant deliberative planning approaches, sometimes combined with local OA planners, have been published. For example, Naeem et al. [15] utilizes the Direction Priority Sequential Selection (DSPP) algorithm, as an extended version of the A* algorithm, that utilizes virtual obstacles to bias the search for a COLREGs-compliant trajectory with increased performance. Similarly, Larson et al. [16] combines Velocity Obstacles (VO) with A* algorithm through utilization of skewed trapezoidal regions of vessels' time-projected positions. Kuwata et al. [5] combines high-level path planning with VO to achieve COLREGs-compliant OA and trailing of a moving target, and integrates it into NASA JPL's CARACaS architecture. Similarly in our previous work [6], we introduced a trajectory planning algorithm for COLREGs-compliant target following that combines deliberative 4D planning and Generalized Velocity Obstacles (GVO) based local planning to compute safe trajectories that respect the USV's dynamics. In these studies, however, the experiments were carried out in rather simple scenarios that allowed search for a collision-free path in real-time.

The primary issue with deliberative approaches are their high computational requirements, especially when planning in higher dimensional state spaces to achieve safer and more efficient trajectories [10]. Hence, in contrast to the previous approaches, we address this challenge by dynamically adapting the resolution of the state space lattice during the search, which results in a significant increase in the performance of our planning algorithm. In addition, our algorithm computes trajectories that consider the probability of collision between civilian vessels whose behaviors are reciprocally influenced not only by the USV's actions but also by their own maneuvers. Lastly, the planner explicitly reasons about the availability of reactive contingency maneuvers in emergency

situations to increase the safety of the USV's operations.

III. PROBLEM FORMULATION

The task for the planner is to compute a collision-free, dynamically feasible, COLREGs-aware trajectory between the current and goal states of the USV in a complex operational scenario with civilian vessels. More formally, given:

- (i.) The continuous state space $\mathcal{X} = \mathcal{X}_\eta \times \mathcal{X}_\nu \times \mathcal{T}$ consisting of states $\mathbf{x} = [\eta^T, \nu^T, t]^T \in \mathcal{X}$, where $\eta = [x, y, \psi]^T \in \mathcal{X}_\eta \subset \mathbb{R}^2 \times \mathbb{S}^1$ is the boat's pose and $\nu = [u, v, r]^T \in \mathcal{X}_\nu \subset \mathbb{R}^3$ is its velocity consisting of the surge u , sway v , and angular r speeds about the z axis in the North-East-Down (NED) coordinate system [17], and t is time.
- (ii.) The current $\mathbf{x}_{U,I}$ and goal $\mathbf{x}_{U,G}$ states of the USV.
- (iii.) The continuous, state-dependent, control action space $\mathcal{U}_c(\mathbf{x}_U) \subset \mathbb{R} \times \mathbb{S}^1$ of the USV in which each control action $\mathbf{u}_c = [u_d, \psi_d]^T$ consists of the desired surge speed u_d and heading ψ_d . This space also includes contingency maneuvers $\mathcal{U}_e(\mathbf{x}_U) \subset \mathcal{U}_c(\mathbf{x}_U)$.
- (iv.) A 3 degree of freedom dynamic model of the USV $\dot{\mathbf{x}}_U = f_U(\mathbf{x}_U, \mathbf{u}_h)$ [6] with actuators that produce thrust and moment by taking \mathbf{u}_h as the control input. This control input is determined by the controller $h_U(\mathbf{x}_U, \mathbf{u}_c, P_U)$, where P_U is the set of its parameters.
- (v.) The geometric region $\mathcal{O}_s = \bigcup_{k=1}^K \mathcal{O}_{s,k} \subset \mathbb{R}^2$, which is occupied by static obstacles.
- (vi.) The civilian vessels $B = \{b_l\}_{l=1}^L$, their estimated states $\{\mathbf{x}_{b_l} | \mathbf{x}_{b_l} \in \mathcal{X}_B \subset \mathcal{X}\}_{l=1}^L$, and the geometric region $\mathcal{O}_b = \bigcup_{l=1}^L \mathcal{O}_b(\mathbf{x}_{b_l}) \subset \mathbb{R}^2$ occupied by the vessels. Each vessel has assigned an intention model $\nu = m_l(c(b_l, O_l), \mathbf{x}_U, \mathcal{X}_B)$ that takes the classification function $c(b_l, O_l)$ as one of the inputs and returns a velocity vector ν of the vessel. The function $c(b_l, O_l)$ returns a binary decision about whether b_l follows COLREGs that is based on its observation history O_l . Furthermore, the parameters ω_t and ω_u are also provided to define the uncertainty in following the trajectory by b_l . The uncertainty is represented as a sequence of bivariate Gaussian probability distributions.

Compute:

A collision-free, dynamically feasible trajectory $\tau : [0, T] \rightarrow \mathcal{X}$ such that $\tau(0) = \mathbf{x}_{U,I}$, $\tau(T) = \mathbf{x}_{U,G}$ and its cost is minimized. Each state $\mathbf{x}_U(t)$ along τ thus belongs to the free state space $\mathcal{X}_{free} = \mathcal{X} \setminus \mathcal{X}_{obs} = \{\mathbf{x}_U(t) | U(\eta_U(t)) \cap \mathcal{O}(t) = \emptyset\}$ for $t \in [0, T]$, where $\mathcal{O}(t) = \mathcal{O}_s \cup \mathcal{O}_b(t)$ and $U(\eta_U(t)) \subseteq \mathbb{R}^2$ is a region occupied by the USV at $\eta_U(t)$.

We assume that civilian vessels follow COLREGs unless the classifier $c(b_l, O_l)$ reports otherwise. We also assume that the USV uses a Kalman filter to estimate its own state and that the states of civilian vessels are either provided through radio communication or estimated using Kalman filtered sensor information collected by the USV.

IV. APPROACH

A. State-Action Space Representation

We compute a discrete and lower-dimensional version of the continuous state space \mathcal{X} resulting in 5D state space \mathcal{S}

in which each state $\mathbf{s} = [x, y, \psi, u, t]^T$ consists of position, heading, surge speed, and time variables. The transitions between the states are dynamically feasible and are selected from a discrete version $\mathcal{U}_{c,d}(\mathbf{s}_U)$ of $\mathcal{U}_c(\mathbf{x}_U)$ (see Fig. 3). A discrete control action $\mathbf{u}_{c,d} = [u_d, \psi_d]^T \in \mathcal{U}_{c,d}(\mathbf{s}_U)$ is internally represented as a set of a finite sequence $\{[x, y, t]^T\}_{i=1}^{L_k}$ of desired positions and arrival times of the USV. The end state of each primitive in the body frame of the USV is selected to be in the center of its corresponding state space cube to preserve the continuity of the trajectory.

The discrete set of contingency control actions $\mathcal{U}_{e,d}(\mathbf{s})$ consists of control actions that combine extreme values of the speed ($u_{d,min}$ and $u_{d,max}$), and heading ($-\psi_{d,max}$, $\psi_{d,0}$, and $\psi_{d,max}$). They are used to compute collision probability of a trajectory (see Section IV-D). They are also an integral part of the trajectory and can be immediately applied in case of any of the civilian vessels breaches COLREGs.

This representation of the state-action space allows deterministic, high-performance search that is compliant with the vehicle's differential constraints. The resolution of the state-action space can be determined by the user of the planner depending upon the complexity of the scene and the dynamic characteristics of the USV.

B. Intention Model of Civilian Vessel

The planner considers reciprocal behaviors of other civilian vessels in response to the USV's maneuvers during the search. We assume that a priori knowledge about the local goals of civilian vessels (e.g., through radio communication or by estimating their mission goals). A civilian vessel b_l is classified to be following or breaching COLREGs using a classification function $c(b_l, O_l)$. The classification function estimates the behavior of b_l to be COLREGs-compliant or COLREGs-breaching by observing its past history of states $O_l = \{\mathbf{x}_{b_l}(t), \mathbf{x}_{b_l}(t-1), \dots, \mathbf{x}_{b_l}(t-\Delta t)\}$, and estimating the size and type of the vessel. The planner then predicts the vessel's future trajectory using an intention model $m_l(c(b_l, O_l), \mathbf{x}_U, \mathcal{X}_B)$ that returns an estimate of the most probable velocity vector ν given the states of the USV (\mathbf{x}_U) and civilian vessels (\mathcal{X}_B) at a particular time instant t .

The planner integrates the intention model of each vessel b_l over time to get an estimate of its future trajectory. We represent the uncertainty in following the trajectory using a bivariate Gaussian pdf $p_{b_l,t}(x, y; \mu_{b_l,t}, \Sigma_{b_l,t})$ that returns the probability of the vessel b_l being at the location (x, y) at the time t . The mean $\mu_{b_l,t} \in \mathbb{R}^2$ and the covariance $\Sigma_{b_l,t} \in \mathbb{R}^{2 \times 2}$ vary in t and depend upon the vessel's dimensions, and surge speed u_{b_l} . The mean of the vessel's position always lay on its predicted trajectory that is computed using the intention model of the vessel. We compute the covariance matrix for different times t as follows.

$$\Sigma_{b_l,t} = \begin{bmatrix} c & -s \\ s & c \end{bmatrix}^{-1} \begin{bmatrix} \alpha_{\Sigma,x} \sigma_x^2 & 0 \\ 0 & \alpha_{\Sigma,y} \sigma_y^2 \end{bmatrix} \begin{bmatrix} c & -s \\ s & c \end{bmatrix} \quad (1)$$

Here, c stands for $\cos(\psi_{b_l})$, s stands for $\sin(\psi_{b_l})$, and σ_x^2 and σ_y^2 are initial variances of the vessel's position as

provided by Kalman filter or determined based on radio communication. The parameters $\alpha_{\Sigma,x} = \omega_{t,x}t + \omega_{u,x}/u_{b_l}$ and $\alpha_{\Sigma,y} = \omega_{t,y}t + \omega_{u,y}/u_{b_l}$ are linearly varied in respect to the vessel's surge speed u_{b_l} and time t , where $\omega_{t,x}$, $\omega_{u,x}$, $\omega_{t,y}$, and $\omega_{u,y}$ are user-specified weights.

C. Calculation of Collision Probabilities

Evaluation of each state requires calculation of several collision probabilities during the search for a trajectory.

Definition 1 ($p_{c,s'}^n$): The collision probability of a control action $\mathbf{u}_{c,d}$ executed from \mathbf{s} to reach \mathbf{s}' . $p_{c,s'}^n$ is calculated as a weighted sum of $p_{c,s',U}$ (see Definition 2) and $p_{c,s',B}$ (see Definition 3) given by $p_{c,s'}^n = e^{-\gamma t_{s',s}}((1 - \omega_{c,U,B})p_{c,s',U} + \omega_{c,U,B}p_{c,s',B})$. Here, $\gamma > 0$ is a discount factor, and $t_{s',s}$ is the total time it takes the USV to arrive to the currently expanded state \mathbf{s} from the initial state \mathbf{s}_I .

Definition 2 ($p_{c,s',U}$): The collision probability of the USV with civilian vessels B . Let $\mathcal{P}_c = \{[x_{b_l,t}, y_{b_l,t}]^T | b_l(x_{b_l,t}, y_{b_l,t}) \cap U(\eta_U^T(t)) \neq \emptyset\}$ be the set of positions at which the civilian boat b_l collides with the USV U at time t , where $U(\eta_U^T(t))$ and $b_l(x_{b_l,t}, y_{b_l,t})$ are geometric regions occupied by the vessel b_l and the USV U , respectively. Then, $p_{c,s',U} = \iint_{\mathcal{P}_c} p_{b_l,t}(x, y; \mu_{b_l,t}, \Sigma_{b_l,t}) dx dy$, where $[x, y]^T \in \mathcal{P}_c$. Similarly, $p_{c,s',B}$ is computed.

Definition 3 ($p_{c,s',B}$): The collision probability between the vessels themselves. The computation of $p_{c,s',B}$ is a challenging task as the positions of all the civilian vessels are normally distributed. In order to maintain the efficiency of the search, we precompute collision probabilities $p_{c,s',i,j}$ between two vessels b_i and b_j through sampling of their bivariate Gaussian probability densities. We compute Euclidean distances between sampled locations of the vessels. The probability of collision $p_{c,s',i,j}$ is then computed as the ratio of the number of the samples with the distance less than a user-specified distance threshold $d_{c,min}$, according to which the vessels are in collision. The computed look-up table inputs discrete values of variances of the vessel 1 and 2 ($\sigma_{x,1}^2$, $\sigma_{y,1}^2$, $\sigma_{x,2}^2$, and $\sigma_{y,2}^2$), the relative position and orientation, and returns the probability $p_{c,s',i,j}$. The collision probability between the vessels is then computed as $p_{c,s',B} = \max_{b_i \in B, b_j \in B, i \neq j} p_{c,s',i,j}$.

Definition 4 ($p_{c,s'}^e$): The collision probability of a contingency control action $\mathbf{u}_{c,e}$ executed from \mathbf{s} to reach a contingency state \mathbf{s}' . $p_{c,s'}^e$ is calculated by taking minimum over the discrete set of contingency control actions $\mathbf{u}_{e,d,i}$ and is given by $p_{c,s'}^e = \min_{\mathbf{u}_{e,d,i} \in \mathcal{U}_{e,d}} p_{c,s',i}^e$.

D. Cost Function

During the search for the trajectory τ , the states are expanded in the least-cost A* fashion according to the cost function $f(\mathbf{s}') = g(\mathbf{s}') + \epsilon h(\mathbf{s}')$. The expected *cost-to-come* between \mathbf{s}_I and \mathbf{s}' is defined as follows.

$$g(\mathbf{s}') = g(\mathbf{s}) + p_s((1 - p_{c,s'}^n)c_{s'} + p_{c,s'}^n((1 - p_{c,s'}^e)c_e + p_{c,s'}^e c_{e,c})) \quad (2)$$

Here, \mathbf{s} is the predecessor of the state \mathbf{s}' being evaluated during the search, $p_s = \prod_{k=1}^K 1 - p_{c,s_k}$ is the probability of reaching \mathbf{s} from \mathbf{s}_I without a collision over K trajectory segments, where p_{c,s_k} is the collision probability of transition between two consecutive states \mathbf{s}_k and \mathbf{s}_{k+1} . The execution cost of $\mathbf{u}_{c,d}$ is $c_{s'} = \omega_n(\omega_c t_{s,s'}/t_{max} + (1 - \omega_c)d_{s,s'}/d_{max}) + c_{-COLREGs}$, where ω_n and ω_c are user-specified weights, $t_{s,s'}$ is the execution time, $d_{s,s'}$ is the length of the control action, and $c_{-COLREGs}$ is the penalty for the state \mathbf{s}' being in a COLREGs-breach region (see Section IV-E). Finally, c_e is the execution cost and $c_{e,c}$ is the collision cost of $\mathbf{u}_{c,e}$.

The *cost-to-go* $h(\mathbf{s}') = \omega_c(t_{s',s_G}/t_{max})(1 - \omega_c)(d_{s',s_G}/d_{max})$ represents a weighted heuristic estimate of the time and distance needed by the USV to transition between \mathbf{s}' and \mathbf{s}_G along a straight trajectory with the maximum surge speed. The parameter ϵ is the inflation factor that balances the search efficiency for the optimality of the trajectory.

E. Evaluation of USV's State for COLREGs Compliance

During the search, the planner determines whether each candidate USV state \mathbf{s} is COLREGs-compliant with respect to all civilian vessels in the scene. First, the conditions $d_{CPA} < d_{CPA,min}$ and $t_{CPA} < t_{CPA,max}$ are used to determine whether the USV at \mathbf{s} is considered to be on a collision course with a civilian vessel. The variable d_{CPA} is the minimum distance between the civilian vessel and the USV along its trajectory for a given time horizon, i.e., the distance from the closest point of approach (CPA) to the civilian vessel [6]. The time to CPA t_{CPA} is the time the USV takes to reach CPA. The constants $d_{CPA,min}$ and $t_{CPA,max}$ are user-specified distance and time thresholds. If the above defined conditions hold, the planner determines the appropriate "give-way" COLREGs rule and evaluates \mathbf{s} for COLREGs compliance as described in [6].

F. Trajectory Search using Adaptive Action Primitives

The search for a dynamically feasible trajectory in a complex 5D state space requires significant computational time, which leads to low replanning frequency. In this section, we introduce a planning algorithm (see Alg. 1) that speeds up the search by time scaling the action primitives based on the estimated collision risk. The collision risk is calculated based on the degree of congestion of the scene which reflects the distribution and density of civilian vessels.

The algorithm exploits the fact that dense sampling is required in regions with a high congestion to compute a high quality trajectory, and can save computational time by sparsely sampling regions with low or no congestion. This substantially increases the efficiency of the search, while preserving the trajectory length and execution time (see simulation results in Figs. 5 and 6).

The performance of the planner is primarily dependent on the prediction of the congestion of the surrounding region around each expanded state \mathbf{s} . The algorithm evaluates the congestion of the scene by calculating $p_{c,s,U}$ (see IV-C) for

each action primitive $\mathbf{u}_{c,d} \in \mathcal{U}_{c,d}(\mathbf{s})$ using estimated future trajectories of civilian vessels (see IV-B). Let $\mathcal{U}_{c,d,free}(\mathbf{s}) \subseteq \mathcal{U}_{c,d}(\mathbf{s})$ be the largest subset of consecutive control actions with $p_{c,s,U}$ below the threshold $p_{c,s,U,min}$ of collision risk at \mathbf{s} , then $\lambda_{cgn} = 1 - |\mathcal{U}_{c,d,free}(\mathbf{s})|/|\mathcal{U}_{c,d}(\mathbf{s})|$ be the degree of congestion for the region around \mathbf{s} . Intuitively, λ_{cgn} provides an approximation of the percentage of the workspace region around \mathbf{s} with a high collision risk.

The time scaling of action primitives in $\mathcal{U}_{c,d}(\mathbf{s})$ is dynamically modified for each state \mathbf{s} being expanded during the search according to the scaling factor m_u . The scaling factor m_u is computed based on λ_{cgn} as shown in Alg. 2. For example, the algorithm gradually increases m_u as it propagates the search tree in state space regions with very low congestion (low values of λ_{cgn}), while it decreases it in regions with high congestion. In addition, when transitioning from a low to high congestion scene, there might be a situation where most of the action primitives expanded by the factor of m_u will lead to collision, i.e., $|\mathcal{U}_{c,d,free}(\mathbf{s})| \approx 0$ and thus $\lambda_{cgn} \approx 1$. In this situation, the algorithm reopens the same state \mathbf{s} that has been already expanded during the search (i.e., it is in the closed set) by adding it to the priority queue (i.e., the open set). The state is then re-evaluated by reducing the scaling factor m_u by half. If the state is reopened and re-evaluated again and λ_{cgn} is close to 1, the algorithm shrinks the scaling factor to its default value $m_u = 1$. In Alg. 1 and 2, the re-evaluation boolean variable is labeled as r .

During the search, the neighboring state \mathbf{s}' of \mathbf{s} is determined using a discrete state transition function $f_{U,d}(\mathbf{s}, \mathbf{u}_{c,d}, m_u) = [x + l_u(m_u - 1)\cos(\psi_d), y + l_u(m_u - 1)\sin(\psi_d), t + (l_u m_u)/u_d]^T$ that inputs the current state \mathbf{s} being expanded, the default control action $\mathbf{u}_{c,d}$, and the scaling factor m_u . Here, (x, y) and ψ_d is the terminal position and heading of the USV after the execution of $\mathbf{u}_{c,d}$ for the time t , respectively, and l_u is the length of the resulting trajectory. The scaling factor is always $m_u \geq 1$. Hence, the scaled control action set $\mathcal{U}'_{c,d}(\mathbf{s})$ guarantees its dynamic feasibility, i.e., its control actions can still be executed by the low level controllers of the USV.

V. RESULTS

A. Experimental Setup

The simulation setup consisted of an experimental scene of 200×200 m, the USV14 (a 4.3 m long catamaran USV as described in [6]), and civilian vessels. We used 6 evaluation scenarios that varied in the number of civilian vessels. For each scenario, we generated 1000 test cases. In each test case, the USV was positioned at its initial state $\mathbf{s}_I = [0, 100, 0, 0, 0]^T$ and directed to move to its stationary goal position $[200, 100]^T$ (i.e., we ignored the heading and surge speed state variables). The civilian vessels were placed in the scene with randomly selected sizes, positions, headings, and surge speeds. They were modeled using a simple car kinematic model with the Ackermann steering geometry [18]. The length of each vessel was randomly selected between 6 and 10 m, the maximum surge speed between 2 to 5 m/s, and the steering angle between 20 and 60 degrees. The

Algorithm 1 COMPUTETRAJECTORY($\mathbf{s}_I, S_G, \mathcal{U}_{c,d}$)

Input: Initial USV's state \mathbf{s}_I , desired goal region S_G , and a default control action set $\mathcal{U}_{c,d}$.
Output: A trajectory τ .
1: Let $S_O \leftarrow \{\mathbf{s}_I\}$ be a priority queue of states sorted in ascending order according to the cost function f (see (2)).
2: Let $S_C \leftarrow \emptyset$ be the set of all expanded/closed states.
3: Let $m_u \leftarrow 1$ be the scaling factor of $\mathcal{U}_{c,d}$.
4: Let $r \leftarrow false$ be the state re-evaluation indicator.
5: **while** S_O not empty **do**
6: $S_C \leftarrow \mathbf{s} \leftarrow S_O.FIRST()$
7: **if** $\mathbf{s} \in S_G$ **then**
8: **return** A trajectory τ generated by recursively tracing the predecessors of \mathbf{s} up to \mathbf{s}_I .
9: **end if**
10: Let $C_U \leftarrow \emptyset$ be the set of collision probabilities of the USV with civilian vessels.
11: **for all** $\mathbf{u}_{c,d} \in \mathcal{U}_{c,d}$ **do**
12: $\mathbf{s}' \leftarrow f_{U,d}(\mathbf{s}, \mathbf{u}_{c,d}, m_u)$
13: **if** $\mathbf{s}' \notin S_C$ **then**
14: Estimate states $\mathcal{X}_{B,t'}$ of all civilian vessels at time t' by forward simulating their intention models $\{m_i\}_{i=1}^{|B|}$. Compute the collision probabilities $p_{c,s'}$ and $p_{c,s'}^e$ (see Section IV-D) for the USV moving between \mathbf{s} and \mathbf{s}' .
15: **if** $(\mathbf{s}' \notin S_O)$ OR $(\mathbf{s}' \in S_O \text{ AND } (f_{new}(\mathbf{s}') < f_{old}(\mathbf{s}'))$ **then**
16: Set \mathbf{s}' as the best successor state of \mathbf{s} .
17: Insert/update \mathbf{s}' into/in S_O .
18: Insert $p_{c,s',U}$ into/in C_U .
19: **end if**
20: **end if**
21: **end for**
22: $\{m_u, r\} \leftarrow \text{COMPUTESCALINGFACTOR}(C_U, m_u, r)$
23: **if** r is true **then**
24: Remove \mathbf{s} from S_C and insert it into S_O .
25: **end if**
26: **end while**
27: **return** $\tau = \emptyset$ (no suitable trajectory has been found).

Algorithm 2 COMPUTESCALINGFACTOR(C_U, m_u, r)

Input: A set C_U of collision probabilities of the USV with civilian vessels for all control actions in $\mathcal{U}_{c,d}(\mathbf{s})$, scaling factor m_u of $\mathcal{U}_{c,d}$, and state re-evaluation boolean indicator r .
Output: A new scaling factor m'_u of $\mathcal{U}_{c,d}$ and the state re-evaluation boolean indicator r' .
1: Let $\lambda_1, \lambda_2, \lambda_3$, and $\lambda_4 \in [0, 1]$ be the user-defined scene congestion levels and $0 < \lambda_1 < \lambda_2 < \lambda_3 < \lambda_4 < 1$. The values of congestion below λ_1 suggest the scene is almost free and values above λ_4 indicate the scene has heavy traffic.
2: Let $\lambda_{cgn} \leftarrow (1 - |\mathcal{U}_{c,d,free}(\mathbf{s})|/|\mathcal{U}_{c,d}(\mathbf{s})|)$ be the scene congestion predictor, where $\mathcal{U}_{c,d,free}(\mathbf{s})$ is the largest subset of consecutive control actions with $p_{c,s',U} \in C_U$ below a user-specified threshold $p_{c,s,U,min}$.
3:

$$m'_u \leftarrow \begin{cases} 2m_u & \text{if } \lambda_{cgn} < \lambda_1 \\ m_u + \delta m & \text{if } \lambda_1 < \lambda_{cgn} < \lambda_2 \\ m_u & \text{if } \lambda_2 < \lambda_{cgn} < \lambda_3 \\ m_u - \delta m & \text{if } \lambda_3 < \lambda_{cgn} < \lambda_4 \\ m_u/2 & \text{if } \lambda_4 < \lambda_{cgn} \text{ and } r \text{ is false} \\ 1 & \text{otherwise} \end{cases} \quad (3)$$

4: $m_u \leftarrow \min(m_u, m_{u,max})$, where $m_{u,max}$ is the user-specified scaling factor threshold.
5: $r' \leftarrow true$ if $\lambda_{cgn} > \lambda_4$, otherwise $r' \leftarrow false$.
6: **return** $\{m'_u, r'\}$

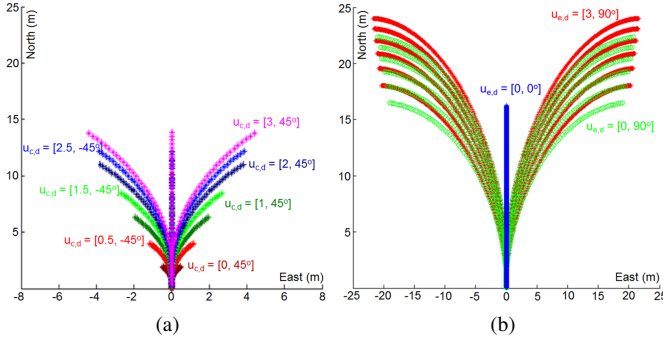


Fig. 3: a) A dynamically feasible control action set $\mathcal{U}_{c,d}$, and b) a dynamically feasible contingency control action set $\mathcal{U}_{e,d}$ for the USV14 with different initial surge speeds.

simulations were performed using on Intel(R) Core(TM) i7-2600 CPU @ 3.4 GHz machine with 8GB RAM.

The set of action primitives used during the search for a trajectory was designed using the 3 DOF dynamics model of the USV14. The heading of the USV14 was discretized into 8 levels and the surge speed into 6 levels ranging from 0 to 3 m/s. Action primitive $\mathbf{u}_{c,d}$ was designed by placing the USV14 at its initial configuration, and then applying a control input $[u_d, \psi_d]^T$ through a PD-controller until the USV14 reached the desired u_d and ψ_d . This resulted in dynamically feasible motion primitives represented as finite sequences of $[x, y, t]^T$ positions, and arrival times. During the search, the state transitions were allowed only between the states with the same or directly adjacent levels of heading and speeds. We also designed 5 dynamically feasible contingency maneuvers $\mathbf{u}_{e,d,1} = [0, 0]^T$, $\mathbf{u}_{e,d,2} = [3, -90]^T$, $\mathbf{u}_{e,d,3} = [0, -90]^T$, $\mathbf{u}_{e,d,4} = [3, 90]^T$, and $\mathbf{u}_{e,d,5} = [0, 90]^T$. During an emergency situation, the USV14 selects a contingency maneuver that leads to the maximum value of d_{CPA} with respect to all civilian vessels.

The parameters of the cost function (see (2)) are $d_{max} = 200$ (i.e., twice the length of a straight trajectory between $\mathbf{s}_{U,I}$ and $\mathbf{s}_{U,G}$), $t_{max} = d_{max}/1.5$ (the average speed of 1.5 m/s), $\omega_n = 1000$, $\omega_c = 0.5$, $c_{COLREGs} = 1000$, $c_e = 500$, $c_{e,c} = 10000$, $\gamma = 0.1$, $\omega_{c,U,B} = 0.3$, and $\epsilon = 4$. The threshold values for CPA parameters used to evaluate USV's states for COLREGs compliance are $d_{CPA,min} = 50$ m and $t_{CPA,max} = 30$ s.

We used Velocity Obstacles (VO) [5] as an intention model $m_l(c(b_l, O_l), \mathbf{x}_U, \mathcal{X}_B)$ to predict a trajectory of each civilian vessel b_l . During the search, we assign the USV14 to each expanded state and forward simulate b_l using VO to capture its reciprocal behavior in response to USV14's action. At every state, VO outputs a velocity vector that the civilian vessel will execute to reach its desired goal position. In order to determine the future projected pose of the vessel, we integrate the velocity vector of the vessel over time it takes the USV14 to reach its next state. This forward projection of the vessel's state was made under the assumption that it will maintain the same velocity vector for the duration of the USV's state transition. The parameters $\omega_{t,x} = \omega_{t,y} = 0.5$

and $\omega_{u,x} = \omega_{u,y} = 1$ of the covariance matrix, that is used to determine 2D Gaussian distribution at each state along the predicted vessel's trajectory, were determined empirically based on the vessel's length, turning radius, and speed.

B. Simulation Results

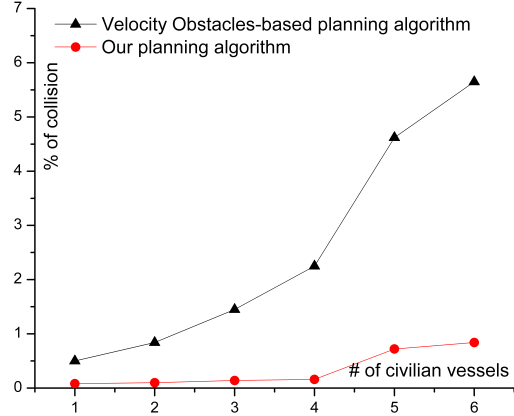


Fig. 4: The percentage of collision test cases for a VO-based reactive planner compared to the developed deliberative planner in combination with the VO-based reactive planner.

We have performed simulation experiments to compare the percentage of scenarios in which the USV14 collided with any of the civilian vessels using VO-based local planner [5] and our deliberative planner in combination with the VO-based reactive planner (see Fig. 4). The plot shows that the rate of collisions for the deliberative planner is significantly lower (i.e 0.7 and 0.8 for 5 and 6 vessels respectively) as compared to the VO-based planner. The VO-based planner does not reason about the motion of all other vessels and does not consider the dynamics of the USV, which leads to a higher rate of collisions. The dynamics of the USV can be considered through the use of the GVO-based planner [6]. However, this would increase the computational demand of the planner. Also, the deliberative planner evaluates the trajectory for the availability of contingency maneuvers, which are executed during emergency situation.

The effectiveness of the developed planner (see Alg. 1) is demonstrated by comparing computational performance of the search with adaptive and constant control action primitives. The table in Fig. 5 shows the statistics of the computational time and the number of expanded states for both the types of the search. The number of states expanded by the search that uses adaptive primitives is at least 5 times less as compared to the search that uses constant primitives. The developed algorithm exploits the fact that all the regions of the workspace are not densely occupied by civilian vessels and dynamically scales the action primitives to sparsely cover these regions, which leads to expanding a significantly less number of states during the search. On the contrary, the algorithm that uses primitives of a constant length unnecessarily expands states in regions with low congestion and thus significantly slows down the search.

Fig. 6 compares the traversal time and trajectory length using both the versions of the planner. The traversal time is

Number of boats	Computational Time (seconds)				Number of expanded states			
	Const		Adaptive		Const		Adaptive	
	mean	std dev	mean	std dev	mean	std dev	mean	std dev
1	3.7	2.01	0.7	0.2	440	256	57	25
2	9.2	11.1	1.6	2.2	612	884	93	124
3	16.3	21.8	2.3	3.1	755	1024	102	146
4	21.8	23.0	3.6	4.1	771	885	128	187
5	29.7	28.6	5.1	5.7	856	826	154	210
6	35.1	29.7	5.7	5.9	915	734	157	230

Fig. 5: Computational time statistics and number of states expanded for the developed trajectory planning algorithm with constant and adaptive control primitives.

approximately the same for both the version up to vessel 4 and has a difference of 3 s for both 5 and 6 vessels scenarios. The traversal distance and the difference in means for both the version of the planner increases with the number of civilian vessels because the USV has to yield to a higher number of vessels and it prefers faster but slightly longer paths. This increase is negligible with respect to the total traversal time and distance. Hence, the developed planner does not take long, easy to compute trajectories (e.g., trajectories that circumvent the entire group of vessels along the boundary of the scene), nor it has long delays by waiting for all the civilian vessels to reach their respective goal locations.

Number of boats	Execution Time (seconds)				Distance travelled (meters)			
	Const		Adaptive		Const		Adaptive	
	mean	std dev	mean	std dev	mean	std dev	mean	std dev
1	83.9	5.8	84.7	3.8	200.2	12.4	200.9	12.1
2	83.6	4.7	84.4	5.9	202.0	13.5	202.6	16.7
3	83.6	5.4	84.8	7.2	203.1	15.0	204.0	19.5
4	83.3	6.8	85.7	10.6	204.1	14.3	208.3	26.3
5	85.4	4.6	88.0	11.1	207.3	13.0	211.4	28.3
6	87.2	8.8	90.9	16.3	210.9	23.7	217.8	40.0

Fig. 6: Traversal time and trajectory length statistics for the developed trajectory planning algorithm with constant and adaptive control primitives.

VI. CONCLUSIONS AND FUTURE WORK

In this paper, we have introduced a trajectory planner that incorporates reciprocal behaviors of a USV and COLREGs-following or COLREGs-breaching civilian vessels directly into the search for an optimal trajectory that minimizes collision risk. We have increased the speed of the search in 5D state space by adaptively scaling the set of dynamically feasible control action primitives. This adaptation is based on the estimated collision rates for each USV's state through active probing of its surrounding state space region. We have carried out simulation experiments to demonstrate the improved search speeds and lower incidence of collisions during the execution of optimal USV trajectories.

In future work, we will consider environmental factors such as wind, currents, and the uncertainty in sensing obstacles during the search. We will also increase the planning efficiency by integrating more efficient replanning algorithm such as Anytime Dynamic A* [19]. Our new planner is

compatible with the system architecture used in physical experiments in the two vessel COLREGs scenarios [6].

ACKNOWLEDGMENTS

This work was supported by the U.S. Office of Naval Research under Grants N00014-11-1-0423 and N00014-12-1-0502, managed by R. Brizzolara and K. Cooper.

REFERENCES

- [1] S. Corfield and J. Young, "Unmanned surface vehicles—game changing technology for naval operations," *Advances in unmanned marine vehicles*, pp. 311–328, 2006.
- [2] P. Švec, A. Thakur, E. Raboin, B. C. Shah, and S. K. Gupta, "Target following with motion prediction for unmanned surface vehicle operating in cluttered environments," *Autonomous Robots*, vol. 36, pp. 383–405, 2014.
- [3] U. Commandant, "International regulations for prevention of collisions at sea, 1972 (72 COLREGs)," *US Department of Transportation, US Coast Guard, COMMANDANT INSTRUCTION M*, vol. 16672, 1999.
- [4] S. Campbell, W. Naeem, and G. Irwin, "A review on improving the autonomy of unmanned surface vehicles through intelligent collision avoidance manoeuvres," *Annual Reviews in Control*, 2012.
- [5] Y. Kuwata, M. Wolf, D. Zarghitzky, and T. Huntsberger, "Safe maritime autonomous navigation with COLREGS, using velocity obstacles," *IEEE Journal of Oceanic Engineering*, vol. PP, no. 99, pp. 1–10, 2013.
- [6] P. Švec, B. C. Shah, I. R. Bertaska, J. Alvarez, A. J. Sinisterra, K. von Ellenrieder, M. Dhanak, and S. K. Gupta, "Dynamics-aware target following for an autonomous surface vehicle operating under COLREGs in civilian traffic," in *IEEE/RSJ International Conference on Intelligent Robots and Systems (IROS'13)*, 2013.
- [7] M. Greytak and F. Hover, "Motion planning with an analytic risk cost for holonomic vehicles," in *IEEE Conference on Decision and Control (CDC/CCC'09)*. IEEE, 2009, pp. 5655–5660.
- [8] P. Švec, M. Schwartz, A. Thakur, and S. K. Gupta, "Trajectory planning with look-ahead for unmanned sea surface vehicles to handle environmental disturbances," in *IEEE/RSJ International Conference on Intelligent Robots and Systems (IROS'11)*, September 2011.
- [9] I. Bertaska, J. Alvarez, S. Armando, K. D. von Ellenrieder, M. Dhanak, B. Shah, P. Švec, and S. K. Gupta, "Experimental evaluation of approach behavior for autonomous surface vehicles," in *ASME Dynamic Systems and Control Conference (DSCC'13)*, Stanford University, Palo Alto, CA, October 21–23 2013.
- [10] C. Tam, R. Bucknall, and A. Greig, "Review of collision avoidance and path planning methods for ships in close range encounters," *Journal of Navigation*, vol. 62, no. 3, p. 455, 2009.
- [11] A. Tan, W. C. Wee, and T. Tan, "Criteria and rule based obstacle avoidance for USVs," in *2010 International Waterside Security Conference (WSS)*, 2010, pp. 1–6.
- [12] M. R. Benjamin, J. J. Leonard, J. A. Curcio, and P. M. Newman, "A method for protocol-based collision avoidance between autonomous marine surface craft," *Journal of Field Robotics*, vol. 23, no. 5, pp. 333–346, 2006.
- [13] L. Perera, J. Carvalho, and C. Guedes Soares, "Intelligent ocean navigation and fuzzy-bayesian decision/action formulation," *Oceanic Engineering, IEEE Journal of*, vol. 37, no. 2, pp. 204–219, 2012.
- [14] Y. Xue, B. Lee, and D. Han, "Automatic collision avoidance of ships," *Proceedings of the Institution of Mechanical Engineers, Part M: Journal of Engineering for the Maritime Environment*, vol. 223, no. 1, pp. 33–46, 2009.
- [15] W. Naeem, G. W. Irwin, and A. Yang, "COLREGs-based collision avoidance strategies for unmanned surface vehicles," *Mechatronics*, vol. 22, no. 6, pp. 669–678, 2012.
- [16] J. Larson, M. Bruch, and J. Ebken, "Autonomous navigation and obstacle avoidance for unmanned surface vehicles," DTIC Document, Tech. Rep., 2006.
- [17] T. Fossen, *Handbook of marine craft hydrodynamics and motion control*. Wiley, 2011.
- [18] S. M. LaValle, *Planning algorithms*. Cambridge, U.K.: Cambridge University Press, 2006, available at <http://planning.cs.uiuc.edu>.
- [19] M. Likhachev, D. I. Ferguson, G. J. Gordon, A. Stentz, and S. Thrun, "Anytime dynamic a*: An anytime, replanning algorithm," in *ICAPS*, 2005, pp. 262–271.